Pergamon

Journal of Structural Geology, Vol. 17, No. 11, pp. 1497 to 1506, 1995

0191-8141/95 $9.50 + 0.00

0191-8141(95)00057-7

Conical drag folds as kinematic indicators for strike-slip fault motion

ALEXANDER BECKER

Ramon Science Center, Institute for Desert Research, Ben-Gurion University, Mizpe Ramon, 80600, Israel

(*Received* 25 *November* 1994; *accepted in revised form* 26 *April* 1995)

Abstract—Conical drag folds are developed in the vicinity of faults where rock sequences with significantly different mechanical properties are subjected to oblique shear. The drag folds formed by passive rotation of a competent bed surrounded by flowing incompetent media. Mesoscale conical drag folds can serve as kinematic indicators. The conical fold axis coincides with the rotation axis of slip, and the angle θ between the small circle of poles to bedding and the conical axis is equal to the angle between the pole to tilted bedding and the rotation axis of slip. The sense of asymmetry of the drag fold reflects the sense of shear. The relationship between conical folding and sense of shear established for the mesoscale can be applied to larger fault zones. For example, the geometry of conical drag folds along with other fault-related structures reveal sinistral strike-slip motion in the Mount Arif area of the Negev.

INTRODUCTION

Determination of direction and sense of slip on faults is a basic requirement of structural analysis. A variety of mesoscale kinematic indicators serves to establish the slip direction. The sense of fault displacement under lower-temperature deformation is commonly determined from grooves and striae, bends, steps, trails, tails and feather fractures (Fleuty 1975, Petit 1987, Ramsay & Huber 1987, p. 509). Most of these kinematic indicators are related to a slickensided fault plane and therefore rely heavily upon the interpretation of polished fault surfaces. A relatively smooth fault plane often marks the margin of a fault zone, separating relatively undeformed wall rocks from a zone of more intensive deformation. Even small faults with less than tens of meters of displacement commonly display breccia or gouge zones on the order of tens of centimeters in thickness. The fault surfaces one observes in the field have been formed during the last episode of fault activity, whereas all former fault planes are now ground into tectonic breccia. Thus, the slip direction determined by kinematic indicators related to fault planes typically shows the last, often very small, portion of displacement. The latter may coincide with the main displacement along the fault, but also may represent a very minor component of shear along the fault surface related to subsequent re-activation (Ramsay & Huber 1987, p. 509). Therefore, relying solely upon fault surface-related kinematic indicators may lead to erroneous conclusions regarding the main displacement along a fault affected by multiple episodes of deformation.

In many cases, a relatively smooth fault plane does not exist at all, and the highly deformed crush and ground rocks of the fault zone are gradually replaced by moderately brecciated layers. In addition, the fault zone rocks may be highly weathered and covered by soil or talus, making them inaccessible for observations. These factors, along with the aforementioned problems associated with relying solely on fault surface kinematic indicators, reveal the importance of focusing attention on fault-related structures in the wall rocks.

The sense of slip along faults may also be inferred from drag folds (Davis 1984, pp. 270–271, Groshong 1988, Twiss & Moores 1992, pp. 57–58). In contrast to the fault zone structures, they are often well exposed and available for study. Drag folding is a distortion of bedding or other layering, resulting from shearing of rock bodies past one another (Davis 1984, p. 270). The drag folds are formed either during initial stages of faulting, or during faulting as a result of resistance to slip or shearing in the vicinity of a fault (Davis 1984, p. 270, Ramsay & Huber, 1987, p. 509, Dennis, 1987, p. 342, Groshong 1988). Drag folds are used to indicate sense of shear on normal and reverse faults, where the intermediate axis of stress is oriented nearly parallel to bedding of the faulted rocks. The drag folds in such cases are typically cylindrical, with the slip direction roughly perpendicular to the cylindrical fold axis. The sense of asymmetry of the drag fold reflects the sense of shear. Such folds are often observed when horizontal strata undergo normal or reverse faulting (Fig. 1a), or when a fault displays either reversal of displacement or overprinting on to pre-folded strata striking parallel to the pre-existing fold axes (Fig. 1b).

A more complicated situation arises when the displacement vector is oblique to the strike or dip of the bedding. Passive rotation of a plane inclined at some angle to the rotation axis produces a conical surface (Houston & Parker 1963, Ramsay 1967, pp. 468–469, Cruden & Charlesworth 1972, Stockman & Spang 1982). If the mechanism of folding is passive rotation of a planar domain of a layer in the flowing ductile media, the final geometry represents a circular conical fold. This conical fold has a conical axis coinciding with the rotation axis of the slip, and the angle θ (Fig. 2) is equal to the angle between the pole to tilted bedding and the rotation axis (Figs. 1c & d). A special case resulting in

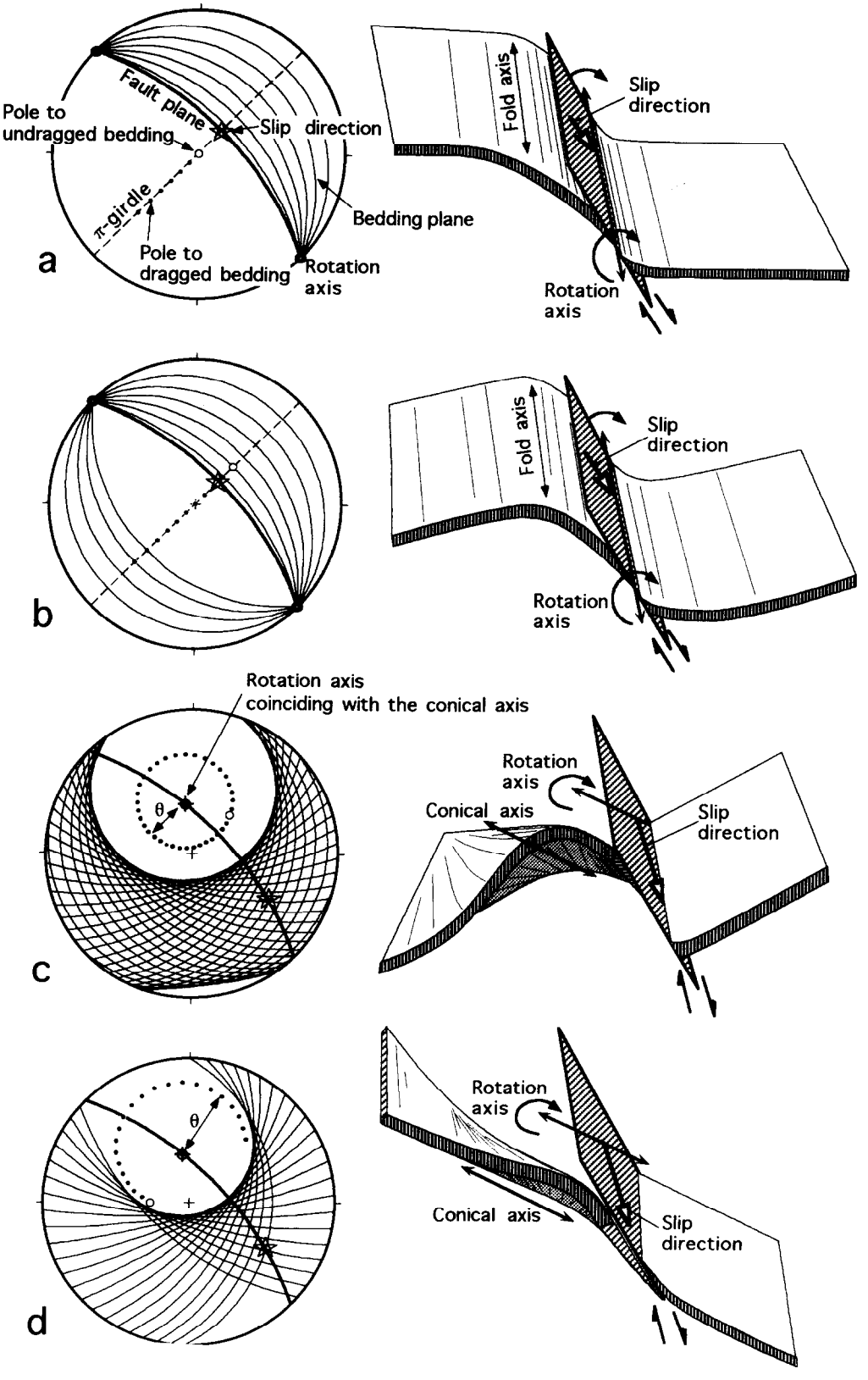

Fig. 1. Drag folds formed by passive rotation of a bed: (a) by normal faulting of horizontal strata: the fold is cylindrical with the fold axis parallel to the rotation axis of slip; (b) by normal faulting of a previously tilted bed: if the rotation axis of slip coincides with the axis of tilting, the fold exhibits cylindrical geometry; (c, d) drag due to oblique slip of a tilted bed; drag folds are conical, the conical axis coincides with the rotation axis of slip, the angle θ is equal to the angle between the pole to tilted strata and the rotation axis. All stereograms are lower-hemisphere, equal-angle projections.

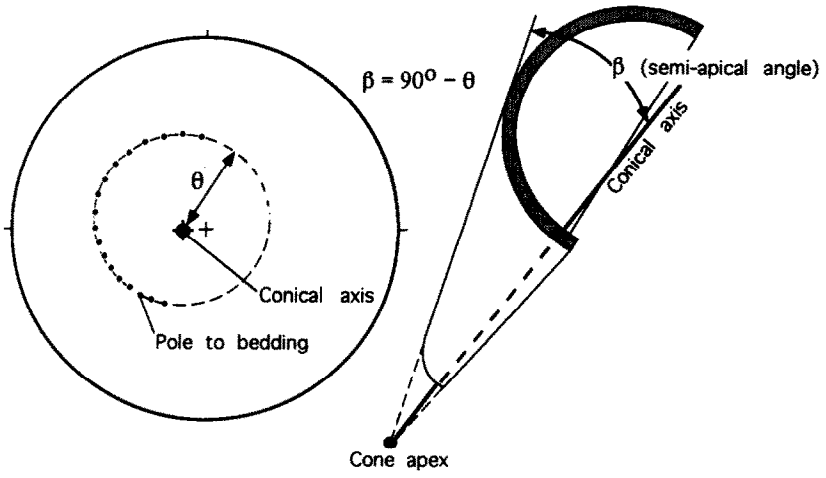

Fig. 2. Geometry of a conical fold.

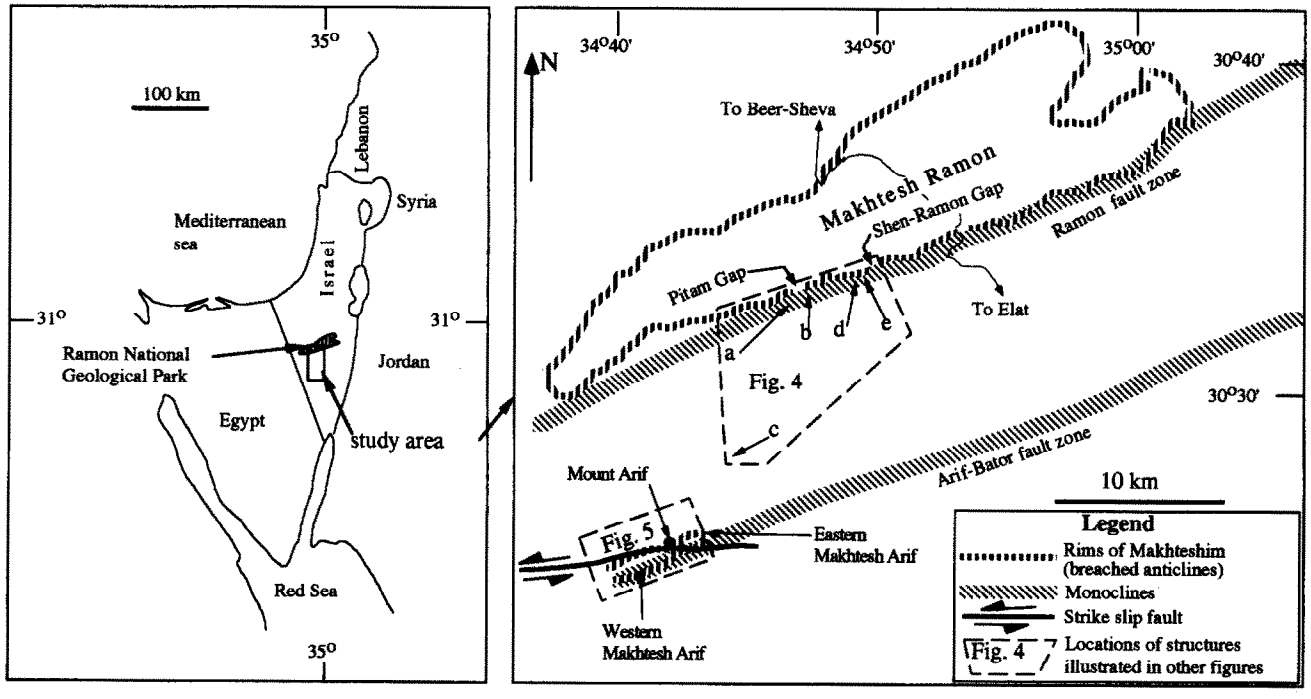

Fig. 3. Location maps of the study areas.

the formation of a cylindrical fold (semi-apical angle is 0°, $\theta = 90°$), occurs upon rotation of a tilted bed around an axis parallel to bedding.

When the flank of a cylindrical fold or a flexure is secondarily folded by passive rotation around an axis oblique to the axis of the pre-existing fold, the final structure represents a dome (or half-dome), which is a combination of a series of conical surfaces (Nicol 1993). Each of these conical surfaces corresponds to the trace of bedding of originally equal attitudes, rotated through various angles about the conical axis.

The geometrical relationships described above are true only in the case of a drag fold outlined by a relatively competent bed that undergoes passive rotation within incompetent ductile media. If a continuous drag fold is developed only by flexural slip, then the fold geometry can not be used to determine sense of slip. Such folds are typically cylindrical and the fold axis lies parallel to the intersection of the bed and the fault plane (Ramsay & Huber 1987, pp. 509–511).

SMALL-SCALE EXAMPLES OF CONICAL DRAG FOLDS

Five folds related to small strike-slip faults have been studied to illustrate the geometrical relationship between drag folds and slip direction. Four folds are located at the southwest margin of the Ramon Fault zone, where strata dip to the southeast or are overturned, dipping northwest. One fold is situated in the area of horizontal strata between the Ramon and Arif–Bator lineaments (Fig. 3). All of the studied folds are drag folds situated along the flanks of small strike-slip faults with offsets ranging from 25 to 60 m. The folds chosen for this study satisfy the following requirements:

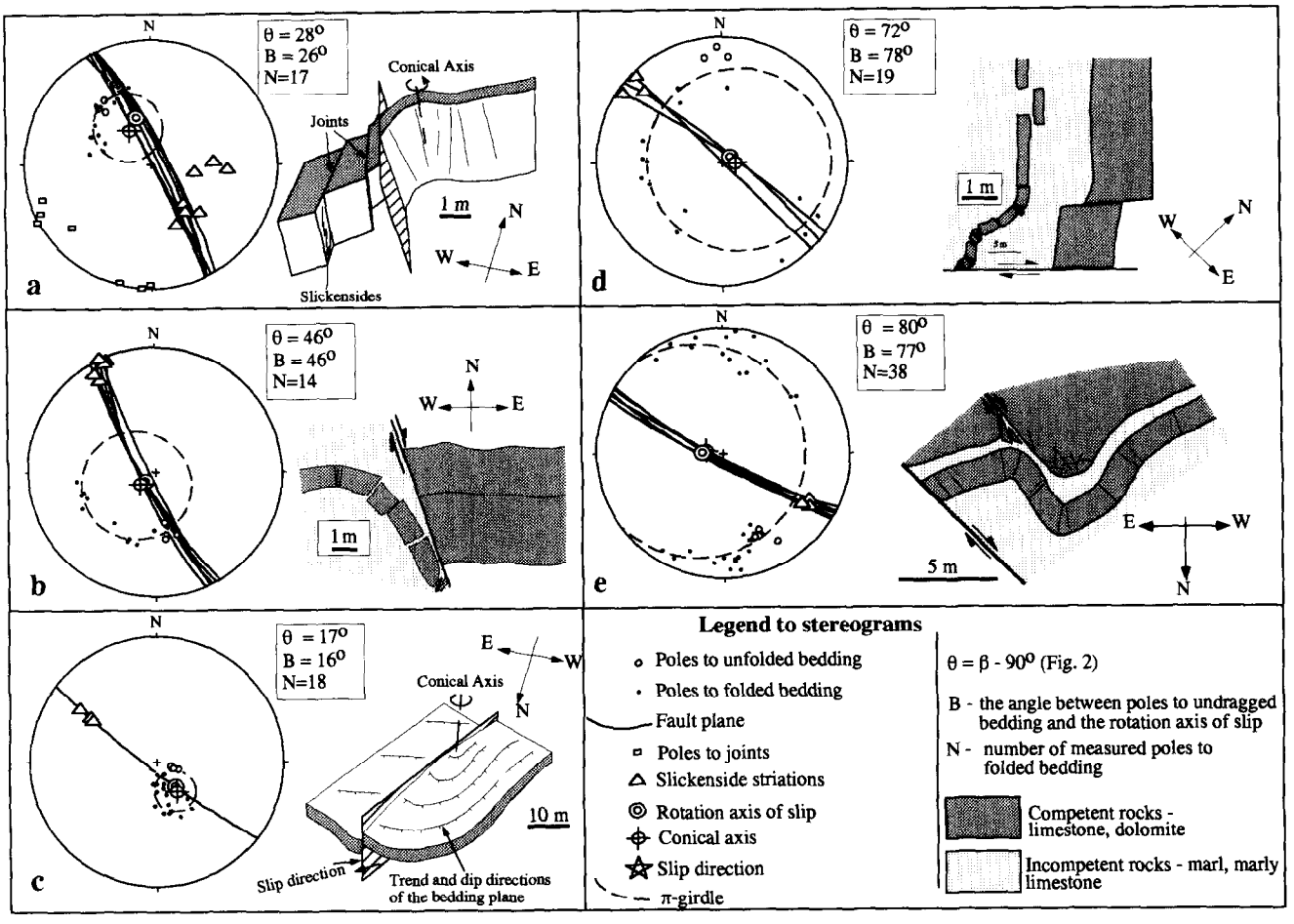

Fig. 4. Geometry of mesoscale conical drag folds, developed in the vicinity of small strike-slip faults. The locations of the folds are shown in Fig. 3.

(1) The fault zones are very narrow (thickness of tectonic breccia and gouge does not exceed 30 cm) and bounded by slickensided fault planes. The faults have small displacements, so there is a high probability that slickenside striations indicate the major displacement direction.

(2) Folded limestone and dolostone beds are surrounded by brecciated marl or shale. Thickness of the brecciated marl is comparable or larger than the thickness of the folded bed.

All of the studied folds (Fig. 4) are located in the Turonian Ora and Gerofit Formations, comprised of interbedded marl, marly limestone, limestone and dolostone. The slip lines were determined by slickenside striae on the fault surfaces (Figs. 4b–e) or by the striae that developed on pre-existing joints which are subparallel to the fault planes and served as small-scale reactivated planes during faulting (Fig. 4a). Slickenside striae are either subhorizontal or moderately inclined.

Drag folds are present only along one flank of a fault. The second flank either does not reveal any deformation (if composed of massive limestone, as in Fig. 4b), or shows multiple shearing of the same sense along pre-existing joints (Fig. 4a). A single hinge could not be identified for the studied folds, thus implying non-cylindrical geometry (Stockman & Spang 1982). Limestone layers did not bend in response to the folding but behaved as discrete blocks bounded by small-scale faults or fractures along the fold. Various degrees of displacement and rotation along these fractures mark the present fold geometry. The displacement was sometimes accompanied by boudinage and pull-apart offsets (Figs. 4b & d), with the open space filled by gouge and breccia derived from adjacent marl and shale units. Many reactivated systematic joints show slickenside lineations that indicate the direction of interblock slip.

The observations described above suggest the following mechanism of conical fold development: a sandwich of limestone and dolostone layers, imbedded in a matrix of marl and shale was subjected to drag during strike-slip faulting. After initial brecciation, the marl and shale lost cohesion and subsequently deformed in a ductile manner. In other words, they underwent cataclastic flow due to fault drag, whereas the limestone and dolostone blocks underwent passive rotation in the flowing media. This rotation was accompanied by boudinage along pre-existing joints confined to limestone and dolostone layers, followed by passive rotation of isolated limestone and dolostone fragments. The former joints acted as small faults bounding the rotating blocks. This process led to the case of rotated fragments that preserve planar contacts, whereas the overall configuration of the resulting structure acquires the geometry of a conical fold (Figs. 4b, d & e).

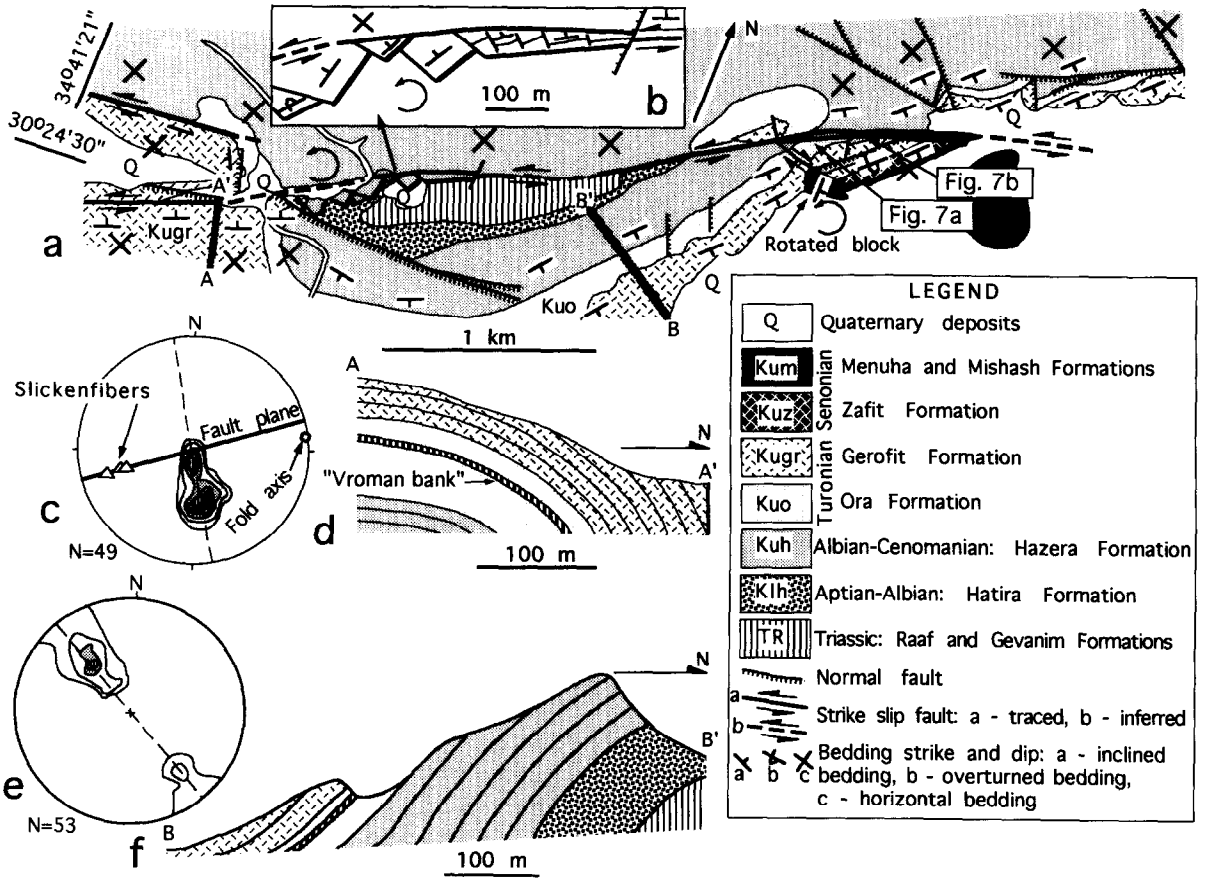

Fig. 5. Geological map and cross-sections of the Mount Arif area: (a) geological map; (b) schematic map view showing the counterclockwise rotated blocks; (c) equal-area projection of poles to bedding of the northward-tilted flexure, contours at 2, 4, 8, 12, 16% per 1% of area; (d) cross-section of the northward-tilted flexure; (e) equal-area projection of poles to bedding of the Arif flexure, contours at 2, 4, 10, 20% per 1% of area; (f) cross-section of the Arif flexure.

Stereograms of poles to bedding (Fig. 4) reveal that the folds appear to be conical, although the poles to bedding are widely scattered about the best fit small circles. The conical geometry is better seen when the semi-apical angle is small ($\beta = 10$–$40°$, $\theta = 80$–$50°$, Figs. 4b, d & e). High values of the semi-apical angle make the pattern less evident (Fig. 4a, and especially Fig. 4c), but in all cases a conical distribution is a better match than a great-circle one.

The conical axis corresponds to the axis of external rotation during faulting. The latter, that lies in the fault plane, was found as the perpendicular to the mean vector of slickenside striations. The angle θ is very close to the angle between the rotation axis and the pole to the unfolded, but previously tilted, bedding in the area.

A MACRO-SCALE EXAMPLE: EVIDENCE FOR A SINISTRAL STRIKE-SLIP AT MOUNT ARIF

Two big conical drag folds have been analyzed in the area of Mount Arif (Fig. 3). The folds are located in the vicinity of a major fault crossing the southwest end of the Arif–Bator lineament at a small angle (Fig. 5a).

The Arif–Bator lineament represents a NE-trending flexure, cut by a set of normal faults. The faults are parallel segments a few km in length, separated by unfaulted intervals. In general the layering strikes northeast parallel to other lineaments of the Syrian Arc (Garfunkel 1978), and ranges from steeply dipping to the southeast to overturned (Figs. 5a & f). The flexure has a cylindrical geometry (Fig. 5e). Multiple angular nonconformities mapped along the Arif–Bator lineament indicate a prolonged structural development. Major nonconformities have been observed at the bases of the Campanian, the Santonian and the Pliocene (Eyal *et al.* 1956, Zilberman 1983).

A dextral strike-slip mechanism has been suggested for the studied fragment of the Arif–Bator lineament by Vroman (1967), Bartov (1974) and Zilberman (1983). This suggestion was originally based on the apparent right-lateral offset of two erosional valleys (makhteshim) at Mount Arif (Vroman 1967). Bartov (1974) suggested that dextral motion along the central Sinai shear zone may extend eastward into the Arif–Bator area, and Zilberman (1983) pointed to the existence of half-dome structures as further evidence for right-lateral strike-slip motion in the area. The present study of drag folds, along with observations of other fault-related structures, lead to the contradictory conclusion of a preexisting flexure at Arif–Bator overprinted by a sinistral strike-slip motion.

Two drag folds are located at the southern slope of Mount Arif, where the major fault crosses the Arif flexure (Figs. 5a and 7). The main fault, situated in between the Cenomanian Hazera Formation and the Turonian Ora Formation, trends SW 220–230° in the area of the first fold (Fig. 7a) and turns to SW 240–250° at the location of the second fold. The fault zone consists of tectonic breccia with sharp angular fragments of limestone and chert, surrounded by fine-grained carbonaceous gouge. The size of the fragments increases northward away from the tectonic contact. The tectonic breccia (a width of 3–5 m) originated from the Hazera Formation. Shale and marl of the Ora Formation in the vicinity of the fault are turned into powder-like gouge and are mostly covered by soil and talus. The contact between the tectonic breccia and the gouge dips 70–85° to the northwest. There is no single relatively smooth fault plane that may be used for structural observations.

The first fold (Figs. 6a and 7a) is outlined by the limestone layers of the 'Vroman Bank'. The 'Vroman Bank' is a bed of fossiliferous limestone (2.7–3.3 m) situated in the upper third of the Turonian Ora Formation (about 50 m thick), composed of shale, marl and marly limestone with some limestone interbeds. The Ora Formation in the area of the fault is overturned and dips 70–80° to NW 295–310°. The drag fold is a convex to the northeast syncline with a circular hinge zone (10–15 m), that does not exhibit a single hinge. The hinge zone is cut by closely spaced (1–5 cm) fractures trending 310–330° and dividing the rock into small tabular fragments. The fold is typically conical: poles to bedding are scattered around a small circle with $\theta = 67°$ (the semi-apical angle β is 23°). The conical axis (plunge 70° to NE 57°) plots near the great circles of the fault planes (Fig. 7a), measured as the contact between the tectonic breccia of the Hatira Formation and the gouge of the Ora Formation. The slip line (plunge 20° to SW 230°) lies on the fault surface, and is normal to the conical fold axis.

The second fold (Fig. 7b) is located 350 m NE of the first one. This fold is found within basal limestone beds of the Gerofit Formation. The 'Vroman Bank' also forms a drag fold here, but it is poorly exposed due to weathering. The angle between the fault plane and the overturned bedding of the Arif Flexure is higher than at the first location, as reflected by the smaller semi-apical angle of the drag fold ($\beta = 16°$, $\theta = 74°$). The conical axis lies in the fault plane (plunge 74° to NW 338°), indicating horizontal sinistral slip.

Folded sigmoidal joints showing sinistral sense of shear have been observed in the area between the two drag folds (Fig. 6b). The well-bedded limestone of the Gerofit Formation dips almost vertically, and the high-angle bedding planes serve as small-scale sinistral shears. Tabular rock fragments bounded by closely spaced systematic joints have been curved to form sigmoidal structures. Unfortunately, the closely spaced sigmoidal joints cannot be measured, but a glimpse of the structures provides insight into the conical fold geometry; the folded joints do not display fold axes parallel to the fracture planes, but rather the hinge zones of northern concave segments plunge in opposite directions to the hinge zones of the southern convex segments.

In the western part of the field area the strike-slip fault is bounded by a flexure with northward-dipping strata (Fig. 5d). The fault zone is covered by stream channel alluvium, but west of the channel the highly deformed limestone crops out. This limestone contains a number of subvertical calcitic veins, trending 260°, parallel to the fault strike. The vein surfaces are covered by slickenfibers plunging 15–25° to WSW. The vertical component of oblique slip resulted in dragging and folding of the strata. The stereogram of poles to bedding (Fig. 5c) demonstrates a preferred orientation along a vertical great circle, indicating a cylindrical structure. The fold axis is horizontal, trending parallel to the fault strike. Here one observes a situation described by Ramsay & Huber (1987, p. 511): the fold axis lies parallel to the line of intersection of the originally horizontal strata and the fault plane. The differences in the fold geometry between the cylindrical flexure and the conical drag folds described above can be explained by the rheological differences of the folded strata. The conical folds formed in a limestone bed surrounded by thick intervals of relatively soft marl and shale. The cylindrical flexure, on the other hand, consists of a well-bedded (0.5–2.0 m) limestone with thin (2–50 cm) interlayer boundaries composed of mechanically weak marl and shale. The thin interlayer boundaries between competent limestone beds did not provide the space necessary for conical fold amplification, thereby resulting in a flexural-slip folding mechanism. Such cylindrical flexures are common at the margins of the strike-slip faults of the Central Sinai shear zone. These flexures often alternate in plunge direction according to undulations of the slip line along the fault strikes (Bartov 1974).

The sinistral strike-slip movement is also corroborated by the geometry of rotated blocks (Fig. 5b), located east of the N-dipping flexure. The strike-slip fault splits into two segments at this locality. The northern segment represents a single fault plane, whereas the southern segment is outlined by the margins of rectangular rotated blocks, and has a zigzag-like shape. Each rotated block consists of strata with a uniform strike and dip. Each block has undergone counterclockwise rotation from its original position. The difference in strike between blocks is significant (up to 40°) and the strike of the blocks is much different from that of the flexure described above.

The northward-tilted cylindrical flexure and counterclockwise rotated blocks support the notion of sinistral strike-slip motion overprinting a pre-existing flexure, matching the conclusion obtained from the geometry of the drag folds. The analysis of conical drag folds indicates that the strata were in the present inclination prior to strike-slip motion. Therefore, the development of the Arif Flexure predated sinistral strike-slip movement. This timing is supported by the presence of multiple angular nonconformities in the Upper Cretaceous sequence along the Arif–Bator lineament.

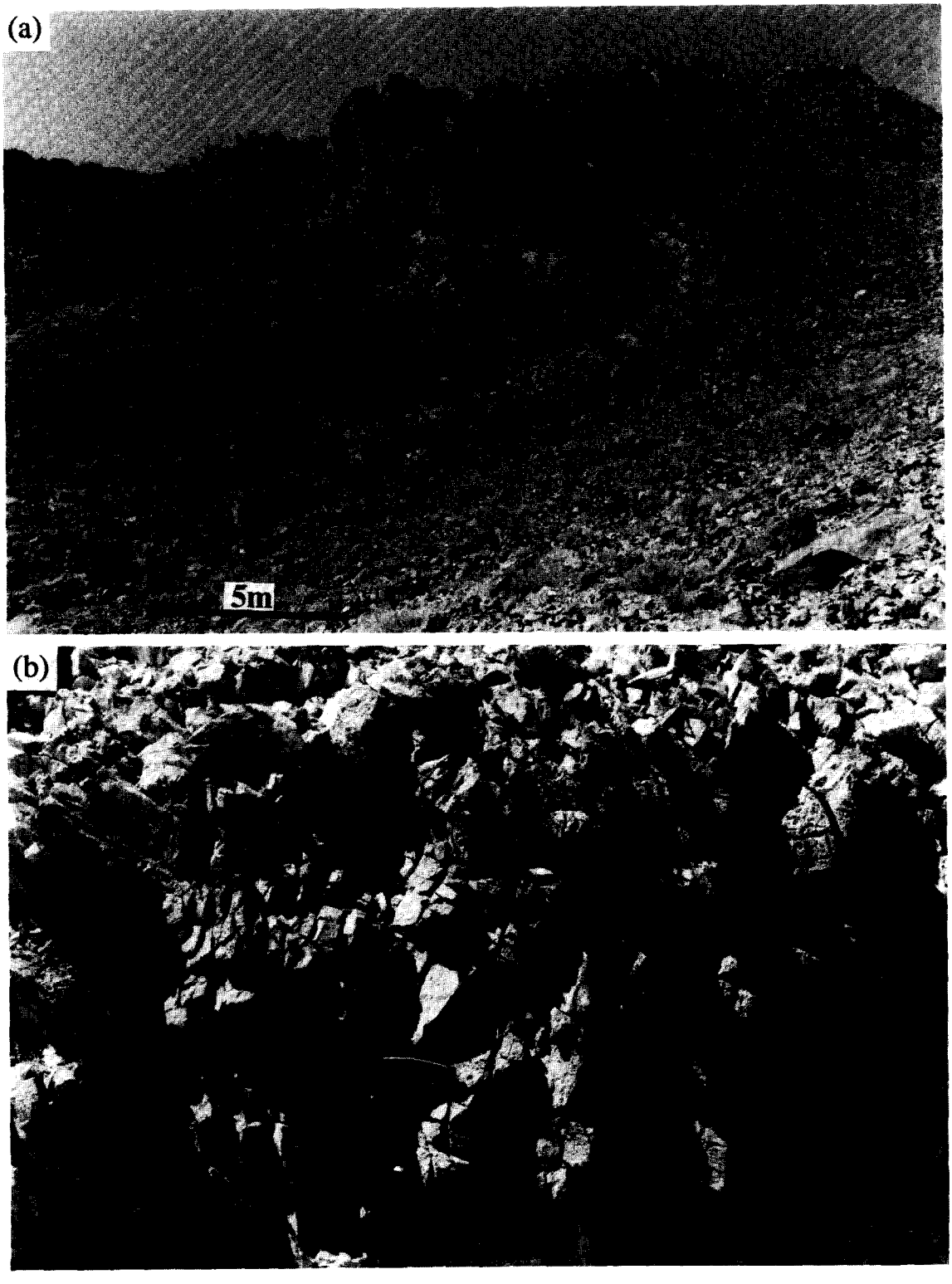

Fig. 6. (a) Photograph of the conical drag fold in 'Vroman Bank' in the vicinity of a sinistral strike-slip fault (looking northeast, fault trace is shown by dashed line). (b) Photograph of sigmoidal (dragged) joints in the limestone of the Gerofit Formation (plan view, north up).

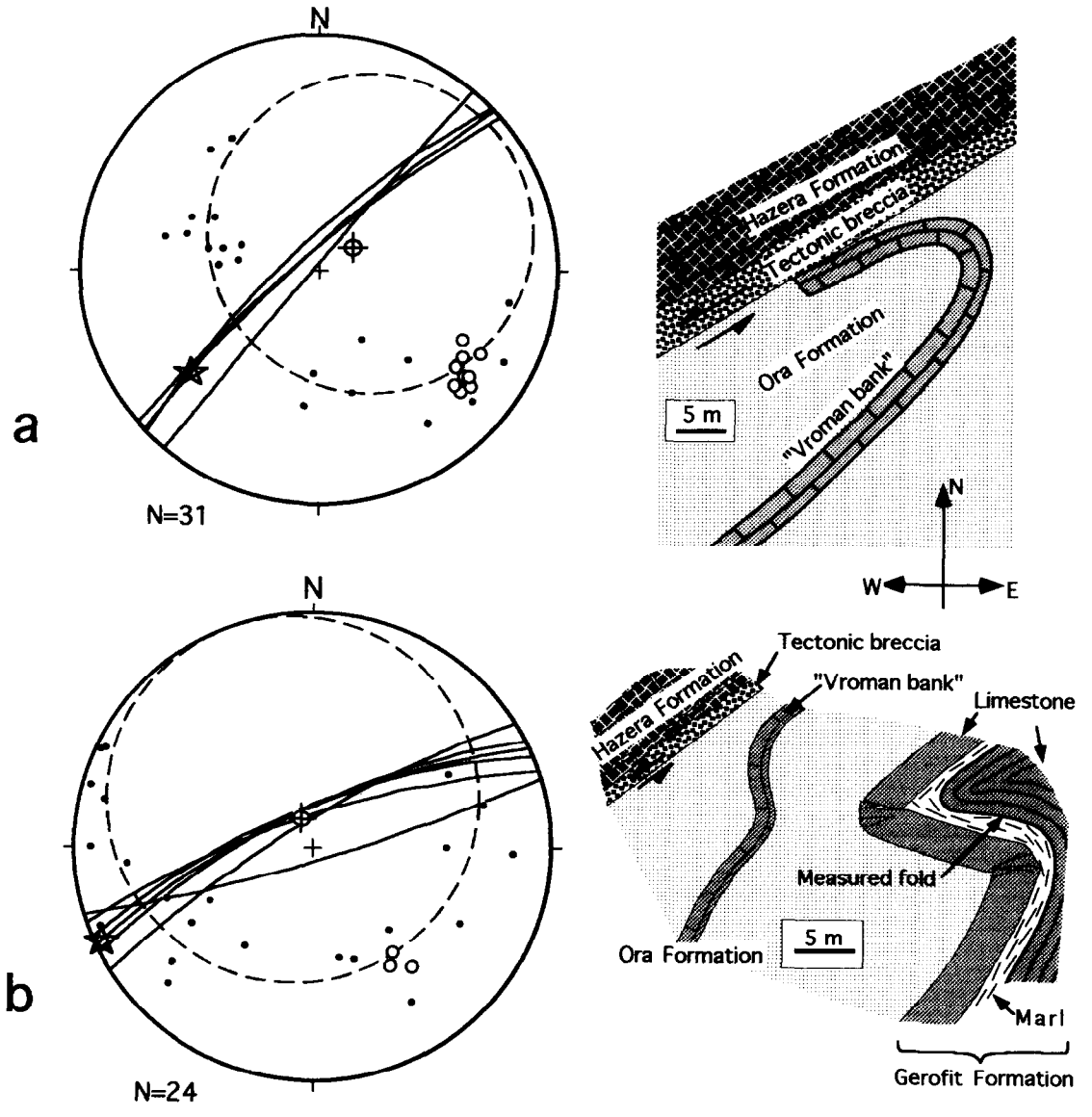

Fig. 7. Geometry of conical drag folds in the vicinity of a sinistral strike-slip fault at the southern slope of Mount Arif. Symbols on the stereograms are the same as in Fig. 4.

DISCUSSION AND CONCLUSION

The examples presented in this study demonstrate that conical drag folds can serve as kinematic indicators. The conical drag folds develop when slip occurs oblique to bedding. Conical axes of drag folds lie in the fault plane perpendicular to the slip line. The angle θ is equal to the angle between the rotation axis of slip and the pole to non-dragged bedding in the area, with fold asymmetry indicating the sense of slip.

Difficulties arise when the semi-apical angle approaches 90°. In such cases, the conical drag fold can be seen in the field, but its axis is difficult to define, due to gentle bedding curvature. This situation was encountered a few times in the field—in such cases it was possible to identify oblique shear, and to roughly determine the shear sense, but the exact orientation of the shear vector could not be obtained.

Another requirement for using drag folds as kinematic indicators is related to stratal composition; to produce a conical fold, volume must be redistributed along fold limbs. A conical fold can form if the hard layer undergoes passive rotation within ductile flowing media. This is possible only when the competent layer is surrounded by incompetent rocks. The flow follows crushing and brecciation of the incompetent units. A continuous fold formed only by flexural slip, without volume redistribution, cannot develop a conical geometry. In cases where volume redistribution is not possible under given pressure–temperature conditions, a cylindrical fold develops instead of a conical fold.

Acknowledgements—Field studies were carried out during geological mapping under financial and technical support from the Ramon Science Center and Geological Survey of Israel. The use of facilities at Ramon Science Center and Geological Survey of Israel is gratefully acknowledged. I wish to thank Michael R. Gross and Emanuel Mazor for their constructive suggestions and improving the English. Peter J. Hudleston, Frederic W. Vollmer and an unknown reviewer are thanked for helpful reviewing of this paper.

REFERENCES

Bartov, I. 1974. A structural and paleogeographic study of the central Sinai faults and domes. Unpublished Ph.D. thesis, Hebrew University, Jerusalem, 143 pp. (In Hebrew, English abstract).

Cruden, D. M. & Charlesworth, H. A. K. 1972. Observations on the numerical determination of axes of cylindrical and conical folds. *Bull. geol. Soc. Am.* **83**, 2019–2024.

Davis, G. H. 1984. *Structural Geology of Rocks and Regions*. Wiley, New York, 492 pp.

Dennis, J. G. 1987. *Structural Geology, an Introduction*. Brown, Iowa, 448 pp.

Eyal, M., Wirzburger, A. & Bartura, Y. 1956. Geological mapping of Makhtesh Arif. *Geol. Sur. Israel, Jerusalem*. 17 pp.

Fleuty, M. J. 1975. Slickensides and slickenlines. *Geol. Mag.* **112**, 319–322.

Garfunkel, Z. 1978. The Negev—regional synthesis of sedimentary basins. *Int. Congr. Sedimentol., 10th Jerusalem Guidebk.* **1**, 35–110.

Groshong, R. H. 1988. Low-temperature deformation mechanisms and their interpretation. *Bull geol. Soc. Am.* **100**, 1329–1360.

Houston, R. S. & Parker, R. B. 1963. Structural analysis of a folded quartzite, Medicine Bow Mountains, Wyoming. *Bull. geol. Soc. Am.* **74**, 197–202.

Nicol, A. 1993. Conical folds produced by dome and basin fold interference and their application to determining strain: examples from north Canterbury, New Zealand. *J. Struct. Geol.* **15**, 785–792.

Petit, J. P. 1987. Criteria for the sense of movement on fault surfaces in brittle rocks. *J. Struct. Geol.* **9**, 597–608.

Ramsay, J. G. 1967. *Folding and Fracturing of Rocks*. McGraw-Hill, New York.

Ramsay, J. G. & Huber, M. I. 1987. *The Techniques of Modern Structural Geology. Volume 2: Folds and Fractures*. Academic Press, London.

Stockman, G. S. & Spang, J. H. 1982. A method for the distinction of circular conical from cylindrical folds. *Can. J. Earth Sci.* **19**, 1101–1105.

Twiss, R. J. & Moores, E. M. 1992. *Structural Geology*. Freeman, New York.

Vroman, 1967. On the fault pattern of Israel and the Levant. *Bull. Isr. Geol. Surv.* **43**, 23–32.

Zilberman E. 1982. The geology of the central Sinai–Negev shear zone, central Negev, Part B. The Arif–Batur lineament. *Geol. Surv. Isr. Rep.* EG/6/83, 58 pp.